Arabian Journal of Chemistry (2017) xxx, xxx–xxx

King Saud University

Arabian Journal of Chemistry

www.ksu.edu.sa
www.sciencedirect.com

ORIGINAL ARTICLE

Electrochemical supercapacitors of cobalt hydroxide nanoplates grown on conducting cadmium oxide base-electrodes

Kailas K. Tehare [a], Manohar K. Zate [a], Sachin T. Navale [b], Sambhaji S. Bhande [a], Sanjay L. Gaikwad [a], Supriya A. Patil [c], Shayam K. Gore [a], Mu. Naushad [d], Sulaiman M. Alfadul [e], Rajaram S. Mane [a,d,*]

[a] *Centre for Nanomaterials & Energy Devices, School of Physical Sciences, SRTM University, Nanded 431606, India*
[b] *Shenzhen University, Nanshan District Key Lab for Biopolymers and Safety Evaluation, College of Materials Science and Engineering, Shenzhen, China*
[c] *Department of Chemistry, Hanyang University, Seongdong-gu, Haengdang-dong 17, Seoul 133-791, Republic of Korea*
[d] *Department of Chemistry, College of Science, Bld#5, King Saud University, Riyadh, Saudi Arabia*
[e] *King Abdulaziz City for Science and Technology, Riyadh 11442, Saudi Arabia*

Received 29 October 2015; accepted 14 January 2016

KEYWORDS

Oxides;
Electrodeposition;
Structural elucidation;
Electrical properties;
Electrochemical properties

Abstract Dopant-free and cost-effective sprayed cadmium oxide (CdO) conducting base-electrodes, obtained at different concentrations (0.5, 1 and 1.5 M), characterized for their structures, morphologies and conductivities by using X-ray diffraction, scanning electron microscopy and electrical conductivity measurements, respectively, are employed as base-electrodes for growing cobalt hydroxide ($Co(OH)_2$) nanoplates using a simple electrodeposition method which further are envisaged for electrochemical supercapacitor application. Polycrystalline nature and mushroom-like plane-views are confirmed from the structure and morphology analyses. Both CdO and CdO–$Co(OH)_2$ electrodes reveal specific capacitances as high as 312 F g^{-1} and 1119 F g^{-1}, respectively, in 0.1 M KOH electrolyte at 10 mV s^{-1} sweep rate. Optimized $Co(OH)_2$–CdO configuration electrode demonstrates energy density of 98.83 W h kg^{-1} and power density of 0.75 kW kg^{-1}. In order to investigate the charge transfer kinematics electrochemical impedance measurements are carried out and explored.

* Corresponding author at: Centre for Nanomaterials & Energy Devices, School of Physical Sciences, SRTM University, Nanded 431606, India.
E-mail address: rsmane_2000@yahoo.com (R.S. Mane).
Peer review under responsibility of King Saud University.

Production and hosting by Elsevier

http://dx.doi.org/10.1016/j.arabjc.2016.01.006
1878-5352

Please cite this article in press as: Tehare, K.K. et al., Electrochemical supercapacitors of cobalt hydroxide nanoplates grown on conducting cadmium oxide base-electrodes. Arabian Journal of Chemistry (2017), http://dx.doi.org/10.1016/j.arabjc.2016.01.006

1. Introduction

Transparent and conducting metal oxides (TCOs) play very important role in developing optoelectronic devices such as solar cells, light emitting diodes, digital displays, and phototransistors, for charge collection purpose (Gulino et al., 2003). Presently, considering higher transparency (⩾90%), 4.8–5.4 eV work function and moderate band gap energies, indium-tin-oxide (ITO) and fluorine-tin-oxide (FTO) are commonly preferred TCOs in optoelectronic devices (Kim et al., 2002). However, the use of sophisticated techniques is unavoidable while developing these TCOs. Secondly, scarcity and expensiveness of indium and tin metals has posed a serious limitation on market feasibility. Furthermore, maintaining both properties (transparency and conductivity) are essentially critical; as conductivity is inversely proportional to transparency. For conductivity improvement it is necessary to (i) modify the metal oxide surface with oxygen plasma, and (ii) develop high quality single crystal structure. Unlike in solar cells, in applications like supercapacitors and fuel cells, transparency of base-substrate electrode is not important. However, in all these applications parameter so called conductivity has considerable impact. It is accepted that ITO is not thermally stable above 300 °C as its resistance increases due to an incorporation of environmental oxygen. Secondly, obtaining commercial-type ITO and FTO, due to limited availability, through chemical methods is practically difficult. Finally, both are expensive for routine daily uses thereby, several efforts have been made to search for alternatives including Zn-doped tin oxide and Cd-doped tin oxide, etc. (Jia et al., 2009). Sprayed boron-doped ZnO conducting and transparent substrates were previously successfully used in dye-sensitized solar cells (Pawar et al., 2009). Cadmium oxide (CdO) films are known for their smaller energy band gaps as compared to other metal oxides such as ZnO, TiO_2, SnO_2, V_2O_5, and WO_3, which are being extensively used in phototransistors, solar cells, gas sensors, infra-red detectors, liquid crystal displays, supercapacitors and anti-reflection coatings, etc. (Waghulade et al., 2007; Kondo et al., 1971). Ordinarily, *n*-type conductivity of CdO is accepted as a result of the non-stoichiometry existing in the cadmium and oxygen. It was assumed that doping with suitable donors could enhance its electrical measurements to be semi-metallic. Till today, several sophisticated chemical and physical methods have been applied for synthesizing CdO thin films in different nanostructures (Yang et al., 2005; Wang et al., 2008; Li et al., 2008; Pan et al., 2001). Consequently, it is worth to develop conducting CdO film which can act as base-electrode for growing another material. On the other hand, due to high specific capacitance (C_s), well-defined electrochemical redox activity and lesser synthesis cost (Yuan et al., 2010; Xia et al., 2011), nanostructures of cobalt hydroxide ($Co(OH)_2$) are enormously been used in electrochemical supercapacitor (ES) application (Wang et al., 2013; Zhao et al., 2011). In literature, various conducting base-substrates have been encountered for growing $Co(OH)_2$ nanostructures including indium-tin oxide (C_s = 1128 F g^{-1}) (Barbieri et al., 2014), stainless-steel (C_s = 860 F g^{-1}) (Gupta et al., 2007), and nickel foam (C_s = 1017 F g^{-1}) (Chang et al., 2007), etc., but, so far there is no report wherein conducting CdO has been used as base-electrode.

In the present investigation, $Co(OH)_2$ nanoplates were grown onto conducting CdO base-electrode by electrodeposition method and applied for ES application. For the first time, chemical spray method was employed to fabricate conducting CdO film as base-substrate for growing $Co(OH)_2$. We do aware of the chemical toxicity of Cd-based materials. However, in continuation to preceding CdO nanostructure-based research (Chang et al., 2007), in the present paper, we made an attempt, for the first time, to use sprayed conducting CdO film electrodes for developing secondary product i.e. $Co(OH)_2$ nanoplates which later were used as electrochemical supercapacitors.

2. Experimental details

2.1. Materials

Cadmium acetate [$Cd(CH_3COO)_2$], cobaltous nitrate [$Co(NO_3)_2$–$6H_2O$], sodium sulfite [Na_2SO_3], etc. were of analytical grade and purchased from Merck Chemicals Ltd. and employed without any further purification. All the used solutions were newly prepared with double distilled water.

2.2. Synthesis of CdO and $Co(OH)_2$

An easy spray pyrolysis method offering effective composition control, homogeneity and uniformity was used for synthesizing conducting CdO films. For synthesizing conducting CdO films, $Cd(CH_3COO)_2$ in different concentrations (i.e. 0.5 M, 1.0 M and 1.5 M) were used. About 5 × 5 cm^2 area glass substrate was used for deposition. These substrate (CdO) films were obtained onto soda-lime glass maintained at 723 K using Cd $(CH_3COO)_2$ precursor solution. The solution dispense rate and gas pressure were 2 ml min^{-1} and 20 kg cm^{-2}, respectively. Compressed air was used as the carrier gas and the nozzle-to-substrate distance was 25 cm. The above parameters were optimized in order to achieve highly homogeneous and adherent CdO films. On spraying the aqueous solution of cadmium acetate over the hot glass substrate, pyrolytic decomposition was obtained, resulting in the formation of CdO film base-electrode. The deposited CdO base-electrode was brownish in appearance, highly adherent and semi-transparent. We believe transparency, application for which these electrodes were used, was not important one. Conductivity of the CdO film was controlled by varying cadmium acetate concentration (0.5, 1.0 and 1.5 M). Deposited CdO films of various conductivities were naturally cooled to room temperature; as the morphology and the electrical properties are highly influenced by the rate of cooling.

The $Co(OH)_2$ nanoplates were grown onto pre-deposited conducting CdO film substrates using electrodeposition method at room temperature. This method has numerous benefits such as it is low temperature deposition method and simplicity of the set up. An electrodeposition process was carried out in a standard three-electrode system in the presence of 0.1 M $Co(NO_3)_2$–$6H_2O$ and Na_2SO_3 in 1:1 volumetric ratio. Platinum wire (in spiral form) was used as a counter electrode and Ag/AgCl was the reference electrode. Deposition was carried out at 4 mA for 300 s. Finally, structural, morphological and electrical studies of obtained $Co(OH)_2$ nanostructures over conducting CdO film electrodes were performed using X-ray diffraction (XRD), field-emission scanning electron microscopy (FE-SEM) and electrical conductivity techniques. For knowing the charge transportation kinetics electrochemical impedance spectroscopy (EIS) plots were measured. Schematic representation of synthesis procedure of conducting CdO and $Co(OH)_2$ nanostructures grown on CdO base-electrode ($Co(OH)_2$–CdO) is illustrated in Fig. 1.

2.3. Characterization details

Structure and morphology of prepared films were analysed by using XRD (Model: Rigaku D/MAX 2500 V) with Cu Kα

Please cite this article in press as: Tehare, K.K. et al., Electrochemical supercapacitors of cobalt hydroxide nanoplates grown on conducting cadmium oxide base-electrodes. Arabian Journal of Chemistry (2017), http://dx.doi.org/10.1016/j.arabjc.2016.01.006

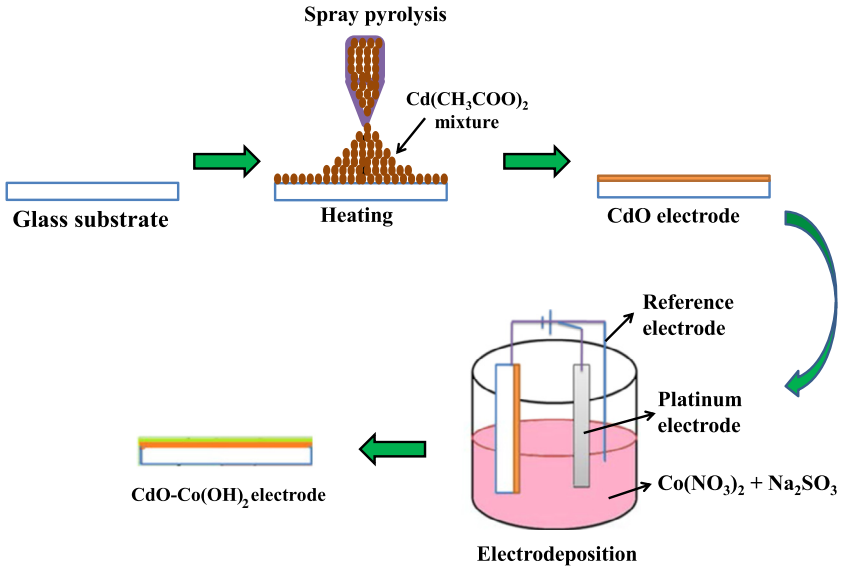

Figure 1 Schematic representation of synthesis of conducting CdO and $Co(OH)_2$-CdO base-electrode.

radiation at $\lambda = 0.154$ nm and FE-SEM (Model: JSM-6700F), respectively. Electrical conductivity measurements of prepared CdO base-electrodes were measured on four probe measurement (SES Inst. Prv. Ltd.) set up. Electrochemical measurements such as cyclic-voltammetry (CV) and galvanostatic charge–discharge (GCD) of as-synthesized CdO base-electrodes and $Co(OH)_2$–CdO electrodes were carried out on a CHI 627B electrochemical analyzer by using typical three electrode system in 0.1 M KOH electrolyte at various scan rate and current densities.

3. Results and discussion

3.1. Morphological, structural and conductivity studies of CdO base-electrodes

Fig. 2(a)–(c) demonstrates the FE-SEM photoimages concerning the plane-views of sprayed CdO electrodes at 0.5 M, 1 M and 1.5 M of $Cd(CH_3COO)_2$ precursor concentrations. Surface morphologies of all the CdO base-electrodes were mushroom-type; quite different from formerly reported morphologies (Goldbarger et al., 2003; Yang and Zeng, 2004; Wang and Li, 2002; Li et al., 2004; Yu and Yam, 2004; Im et al., 2004; Ou et al., 2011). The spacing between two adjacent mushrooms decreased with an increase in $Cd(CH_3COO)_2$ concentration, signifying agglomeration potential of crystallites is a function of precursor concentration. It is worthwhile to mention here is that due to a poor adhesion CdO film was peeling-off from the glass substrate at higher $Cd(CH_3COO)_2$ concentrations (>1.5 M). Cross-sectional FESEM images of CdO film substrates prepared for 0.5 M, 1.0 M and 1.5 M concentrations are shown in Fig. 3(d)–(f). Thicknesses of the prepared CdO films at 0.5 M, 1.0 M and 1.5 M concentrations were 690, 750 and 812 nm, respectively. Fig. 3(a) shows the XRD spectra for CdO film electrodes deposited at different $Cd(CH_3COO)_2$ concentrations (i.e. 0.5 M, 1 M and 1.5 M). The XRD patterns in Fig. 3(a) showed well-defined reflection planes which were matching well with the standard JCPDF (No.: 05-0640) file of CdO, indicating the formation of CdO without any impurity. Crystallite sizes, calculated by using well-known Scherrer's relation along highly oriented (200) peak, were 15, 16 and 27 nm for 0.5, 1 and 1.5 M precursor concentrations, respectively. Slight broadening, in peaks, was noticed confirming infinitesimal change in grain size with concentration, consistent to FE-SEM results. To investigate the conductivity change, current density–voltage measurement tests were performed over three CdO base-electrodes in the range of 2–9 V at $1 \times 1\ cm^2$ electrode surface area and obtained results are displayed in Fig. 3(b). During each measurement ohmic contacts were established. All the current–voltage plots were linear demonstrating good conductivity; however, a slight change in their slopes was evidenced, indicating infinitesimal variation in conductivity as a function of cadmium source concentration. Surface conductivity increased from 2.0 to 5.71 mho cm^{-2} and activation energy decreased from 0.34 to 0.29 eV with increase in cadmium concentration from 0.5 to 1.5 M. We believe that our base-electrodes were partially transparent which practically had no impact on the present study, but exhibited conductivities comparable to other routinely used electrodes (0.22 mho cm^{-2}-ITO, 2.3 mho cm^{-2}-FTO and 7.49 mho cm^{-2}-stainless-steel, etc.), demonstrating significance of sprayed CdO as base-electrode. The existence of shallow donors caused by intrinsic interstitial cadmium atoms and oxygen vacancies might responsible for high conductivity in CdO base-electrode.

3.2. Morphological evolution and structural elucidation of $Co(OH)_2$–CdO electrodes

The XRD patterns of $Co(OH)_2$–CdO electrodes are shown in Fig. 4(a). The only difference was the conductivity of CdO base-electrode. The XRD peaks located at $2\theta = 18.57°$, 35.45°, 45.30° and 58.30° well-matched with $Co(OH)_2$ JCPDF data file no. 45-0031 having Braggs reflections (022), (004), (030) and (312), respectively. While, the other detected peaks at $2\theta = 33.16°$ and 55.30° were due to the CdO base-electrode

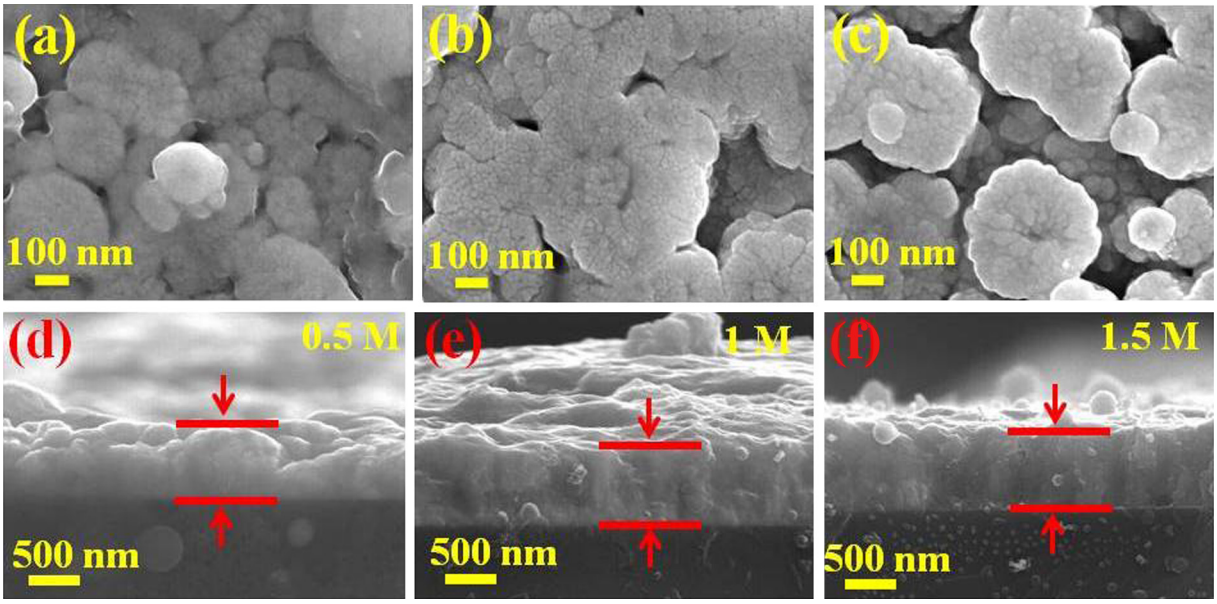

Figure 2 FE-SEM images of; (a–c) plane and cross-sectional views of CdO films prepared at 0.5, 1.0, and 1.5 M cadmium acetate concentrations.

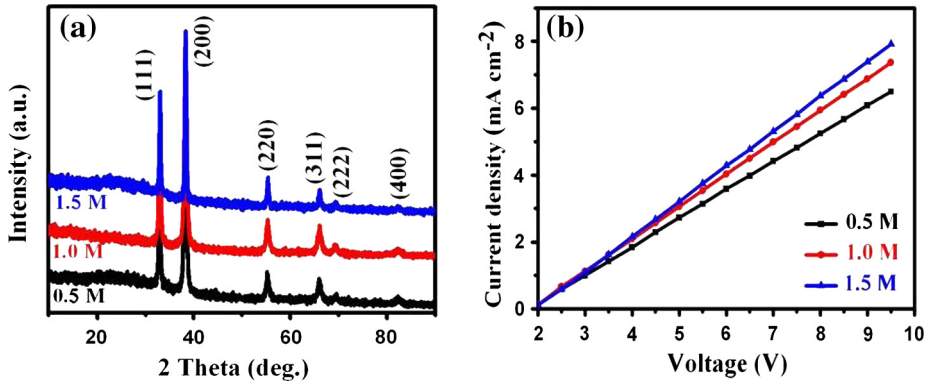

Figure 3 (a) XRD spectra, and (b) conductivity of CdO base-electrodes obtained at 0.5, 1.0 and 1.5 M cadmium acetate concentrations.

(JCPDF file no. 05-0640). No other impurity peaks were detected. Plane-views of $Co(OH)_2$ grown onto CdO base-electrodes of different Cd-concentrations (0.5 M, 1 M and 1.5 M) are shown in Fig. 4(b)–(d). It was observed that at lower concentrations (0.5 and 1.0 M) $Co(OH)_2$ nanoplates just begun to grow. As mentioned previously and novelty of work, CdO electrode (film) of best conductivity was used as base-substrate for depositing $Co(OH)_2$. Basically, because of the conducting nature of CdO deposition of $Co(OH)_2$ happened as for electrodeposition process use of conducting substrate is an essential criteria. During application of external voltage or current, ions of opposite charges migrate across the electrolyte and external circuit by producing a film of desired product. In short, in the present case CdO film acted as base conducting substrate so as to apply current for depositing $Co(OH)_2$ in the presence of platinum cathode. At initial stage, upright-standing free nanoplates were not clearly seen. While for 1.5 M Cd-precursor concentration-based electrode, upright-standing free nanoplates with a large porosity were confirm. Such kind of porous morphology generally is preferred for supercapacitor application because it provides more surface area and open space for the electro-active species, which enhances the electrode–electrolyte area (Liao et al., 2013; Xu et al., 2008, Chang and Hu, 2004; Tao et al., 2011).

4. Electrochemical measurements

4.1. CV and GCD measurements

Electrochemical properties such as CV and GCD of as-deposited $Co(OH)_2$–CdO films as working electrodes were performed in an optimized 0.1 M KOH electrolyte for supercapacitor application. CV measurements of CdO base-electrodes were carried out by using three-electrode system at 10 mV s^{-1} sweep rate (with wide window −0.2 to 0.8 V) and are displayed in Fig. 5(a). From Fig. 5(a) it is observed that with increase in precursor concentration area under the curve increased as well as the redox peaks were evidently seen indicating pseudocapacitor behaviour. Also the value of maximum current (I_{max})

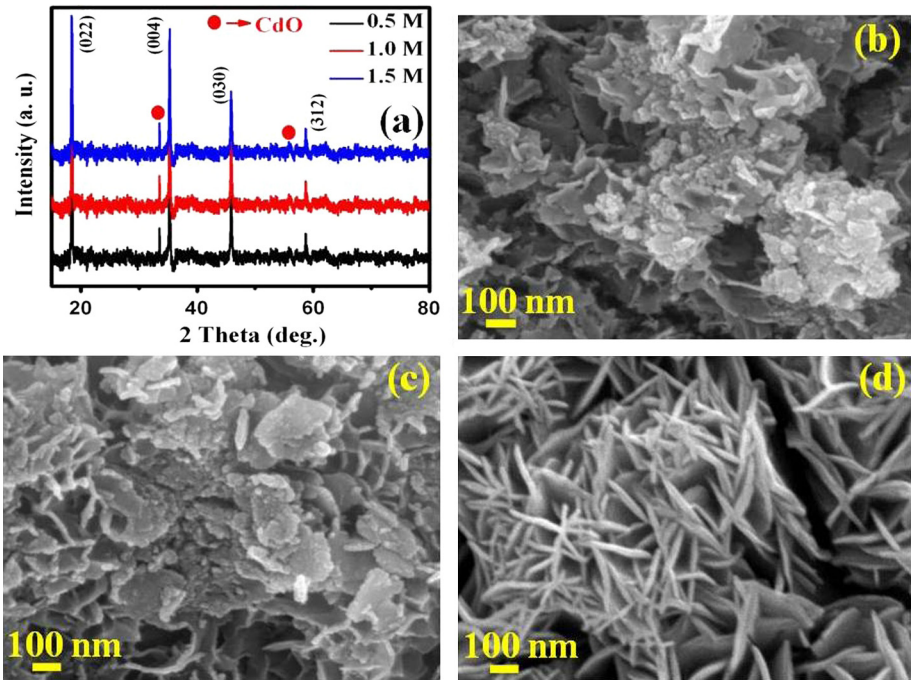

Figure 4 (a) XRD spectra, and (b) plane-view FESEM images of $Co(OH)_2$ nanostructures grown onto CdO base-electrodes of Fig. 2(a)–(c).

increased from 0.3 mA cm^{-2} (for 0.5 M) to 0.44 mA cm^{-2} (for 1.5 M); implying increase in specific capacitance with concentration of Cd-precursor. Fig. 5(b) shows the CV curves of $Co(OH)_2$ grown on CdO base-electrodes at 10 mV s^{-1} sweep rate with −0.2 to 0.8 V potential window. Area under curve in case of 1.5 M concentration was higher as compared to 0.5 and 1 M concentrations. Presence of different redox peaks in CV suggesting influence of CdO base-electrode conductivity on specific capacitance of $Co(OH)_2$–CdO electrodes. Also from Fig. 5(b), a higher specific capacitance (for 1.5 M; which explained in detail further) anticipated on account of upright-standing free $Co(OH)_2$ nanoplate-type morphology which in general facilitates fast penetration of the electrolyte ions into the active $Co(OH)_2$ nanoplates. The C_s values of electrodes from GCD curves were calculated by using the following formula:

$$C_s = \frac{\mathbf{I} \times \Delta\mathbf{t}}{m \times \Delta\mathbf{V}} \quad (1)$$

where '**I**' is the discharge current in Ampere, '**Δt**' is the discharge time in second, '*m*' is the active mass of the electrode material in gram and '**ΔV**' is the potential window in volt. GCD curves of CdO and $Co(OH)_2$–CdO electrodes are shown Fig. 5(c) and (d), respectively at fixed current density of 8 mA cm^{-2}. Charging–discharging behaviour was identical in both the cases. Increase in discharging time with respect to Cd-precursor concentration can be clearly seen from Fig. 5 (c) and (d). Discharging times for CdO electrodes were found to be 78, 96 and 113 s for 0.5, 1, and 1.5 M concentrations, respectively. C_s values of CdO electrodes calculated from Eq. (1) were 249, 278 and 312 Fg^{-1} for 0.5, 1 and 1.5 M Cd-recursor concentrations, respectively at 10 mV s^{-1} scan sweep. GCD curve of $Co(OH)_2$–CdO electrodes for different Cd-precursor concentrations is shown in Fig. 5(d).

The charging time of $Co(OH)_2$–CdO electrodes were 452, 549 and 641 s, while the discharging times were 377, 405 and 449 s, respectively for 0.5, 1 and 1.5 M Cd-precursor concentrations. For discharging, due to an internal resistance and a capacitive component variations the voltage was slowly dropped (Zhang et al., 2012). Calculated C_s value for $Co(OH)_2$–CdO electrodes were 937 Fg^{-1}, 1005 Fg^{-1} and 1119 Fg^{-1} for 0.5, 1 and 1.5 M Cd-precursor concentration, respectively. This relatively higher C_s (1119 Fg^{-1}) value for 1.5 M Cd-concentration electrode was mainly due to its higher conductivity (Fig. 3(b)). The graphical representation of specific capacitance values, obtained from Fig. 5(c) and (d), is shown in Fig. 5(e). Furthermore, nanoplate-like structure of $Co(OH)_2$–CdO electrode (Fig. 4(d)) might provide more surface area for electrolyte diffusion and fast and easy transportation of electrons. Also, from literature it was clear that CdO itself contribute its own specific capacitance (Xia et al., 2011) that might add in $Co(OH)_2$–CdO. When $Co(OH)_2$ grown onto CdO base-electrodes of different conductivities, these electrodes showed higher specific capacitances. It was due to contributions of the base-electrode (conducting CdO) and the $Co(OH)_2$ nanoplates, which was undoubtedly comparable to other reported values for $Co(OH)_2$ nanostructures only (Cao et al., 2004; Chang et al., 2010; Gupta et al., 2007). This corroborated that the CdO film electrode obtained onto glass substrate could serve as a potential working electrode and opened a new avenue for depositing variety of nanostructures of either metal oxides or hydroxides, which is a topic of ongoing work. Long term cyclic stability is essential for practical application of supercapacitor. Cyclic stability of $Co(OH)_2$–CdO electrode (1.5 M concentration) in 0.1 M KOH electrolyte measured at 10 mV s^{-1} sweep rate is presented in Fig. 6(a). Due to the loss of active material caused by the dissolution and/or detachment in the electrolyte, decrease in the specific capacity with number

Please cite this article in press as: Tehare, K.K. et al., Electrochemical supercapacitors of cobalt hydroxide nanoplates grown on conducting cadmium oxide base-electrodes. Arabian Journal of Chemistry (2017), http://dx.doi.org/10.1016/j.arabjc.2016.01.006

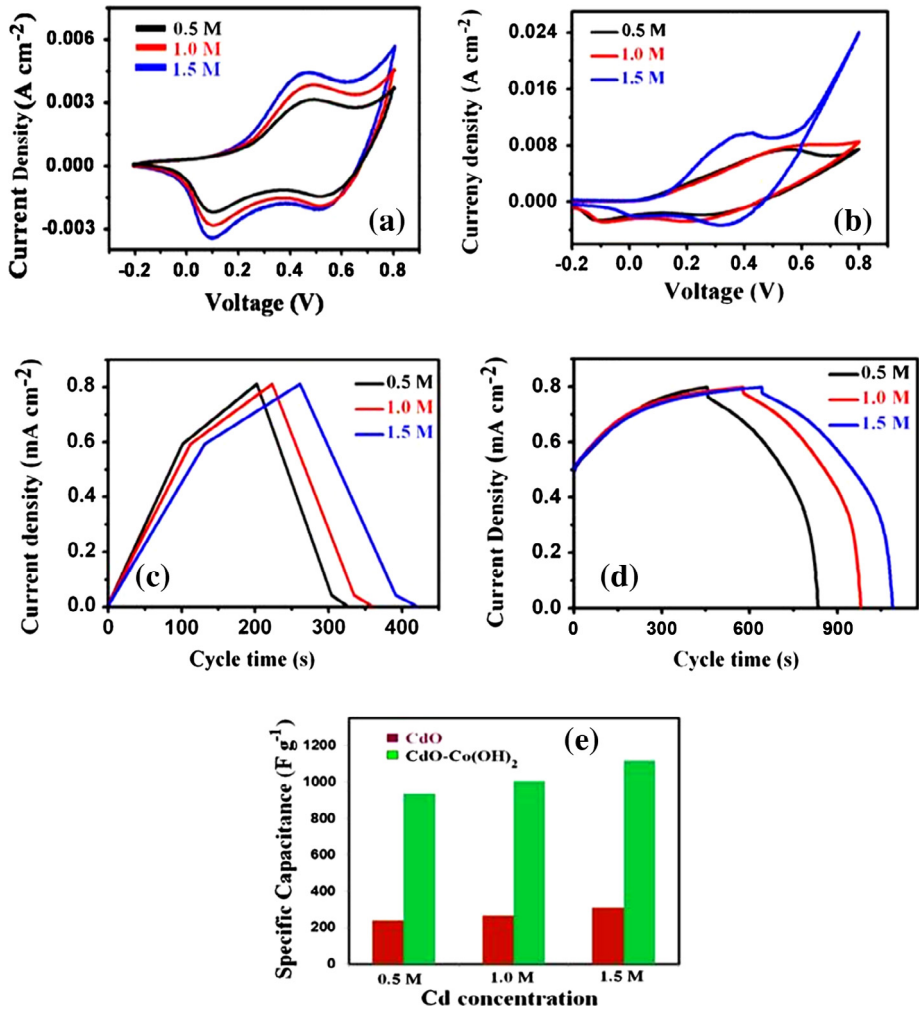

Figure 5 (a and b) Cyclic-voltammograms, and (c and d) charging–discharging curves of CdO and $Co(OH)_2$–CdO electrodes. (e) Graphical representation of specific capacitance values obtained from Fig. 5(c) and (d).

of cycles was observed. After 1000 cycles, C_s value of $Co(OH)_2$–CdO electrode retained 54% of its original value.

4.2. Energy and power densities

From the practical and commercial views of supercapacitor energy and power densities are considered as crucial factors. Energy density (**E**) and power density (**P**) were calculated with the help of following equations (Wu et al., 2010):

$$\mathbf{E} = 0.5 \times \boldsymbol{C}_s \times \Delta \mathbf{V}^2 \quad (2)$$

$$\mathbf{P} = \frac{\mathbf{E}}{\mathbf{T_d}} \quad (3)$$

where '**E**' is in W h kg^{-1}, '**P**' is in kW kg^{-1}, '**ΔV**' refers to potential window during the discharge process in volt and '$\mathbf{T_d}$' is discharging time.

Values of **E** and **P** were calculated for all electrodes and tabulated in Table 1. Conducting CdO electrodes demonstrated lower energy densities (from 22.13 to 27.55 W h kg^{-1}) and higher power densities (from 1.02 to 0.87 kW kg^{-1}). On the other hand, $Co(OH)_2$–CdO electrode of optimal conductivity (1.5 M Cd-precursor concentration) showed as high as energy density of 98.83 W h kg^{-1} and good power density of 0.75 kW kg^{-1}. Based on the obtained electrochemical results it was concluded that, $Co(OH)_2$–CdO electrode, developed at 1.5 M Cd-precursor concentration exhibited excellent capacitive performances than the other concentrations, indicating its potential as a base-electrode material in supercapacitor application.

4.3. Electrochemical impedance analysis

In order to examine the internal resistance and charge transfer kinematics, EIS measurements were carried out. Fig. 6(c) shows the Nyquist plots of $Co(OH)_2$–CdO electrodes at different Cd-precursor concentrations in the frequency range of 100 kHz to 1 MHz with an ac signal of 1 mV amplitude. Very small semicircle in high frequency area and a line in the lower frequency area were confirmed in Nyquist spectra. Small semicircle not visualised in the Nyquist spectra suggested that all the electrodes were holding lower charge transfer resistance. It showed relatively higher charge transfer resistance for 0.5 M Cd-precursor concentration and lower for 1.5 M Cd-precursor

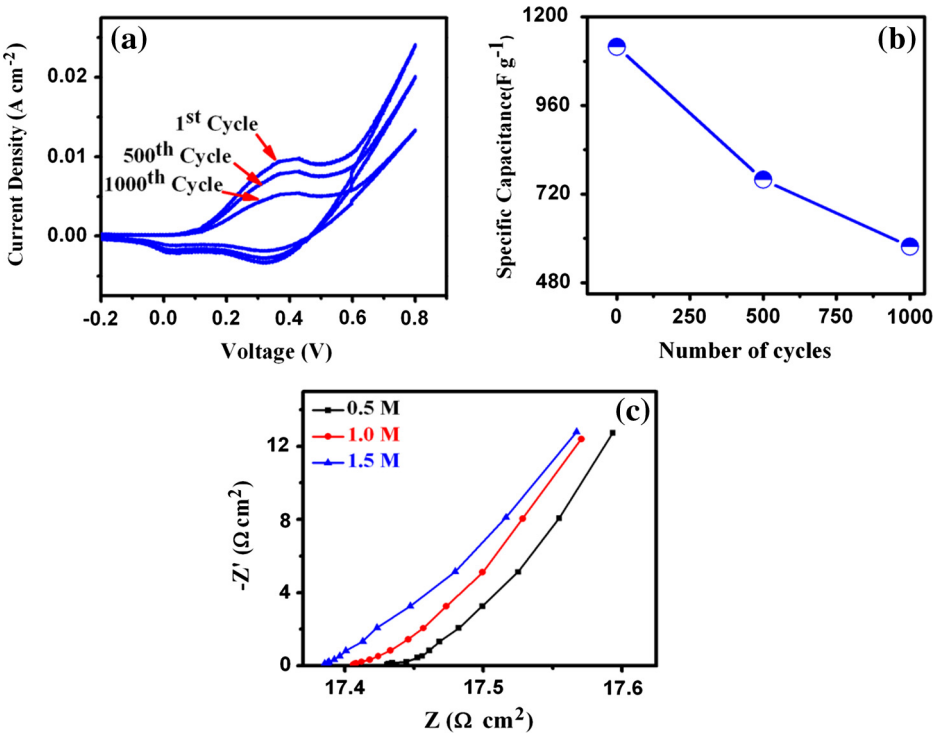

Figure 6 (a) Cyclability of optimized $Co(OH)_2$–CdO electrode, (b) variation of the specific capacitance as a function of number of cycles, and (c) EIS spectra of $Co(OH)_2$–CdO electrodes (base-electrodes prepared at 0.5, 1.0 and 1.5 M cadmium acetate concentrations).

Table 1 Energy and power densities of CdO and $Co(OH)_2$–CdO electrodes.

Electrode	Energy density (W h kg^{-1})	Power density (kW kg^{-1})
CdO (0.5 M)	22.13	1.02
CdO (1.0 M)	24.71	0.92
CdO (I.5 M)	27.55	0.87
$Co(OH)_2$–CdO (0.5 M)	82.75	0.79
$Co(OH)_2$–CdO (1.0 M)	88.76	0.77
$Co(OH)_2$–CdO (1.5 M)	98.83	0.75

concentration, implying that electrochemical supercapacitors performance of $Co(OH)_2$–CdO electrode was Cd-precursor concentration dependent.

5. Conclusions

In summary, synthesis of dopant-free conducting CdO film base-electrodes of mushroom-like surfaces was carried out by varying cadmium acetate concentration (from 0.5 to 1.5 M) on glass substrate using spray pyrolysis method. On these conducting CdO base-electrodes upright-standing $Co(OH)_2$ nanoplates were grown by a simple electrodeposition method and applied for pseudocapacitor (supercapacitor) application. Electrochemical measurements of $Co(OH)_2$–CdO electrode at 1.5 M Cd-concentration demonstrated C_s value as high as 1119 F g^{-1} at 10 mV s^{-1} as well as rate capability together in CV and GCD measurements. After 1000 cycles, C_s value of $Co(OH)_2$–CdO (1.5 M) electrode retained 54% of its original value of capacitance as well as exhibited high energy density of 98.83 W h kg^{-1} with power density of 0.75 kW kg^{-1}. Undoubtedly, the use of conducting CdO base-electrode would open a new potential for energy storage device where conducting thin film counter electrodes are required in contrast to conventional bulk current collectors.

Acknowledgement

This project was supported by King Saud University, Deanship of Scientific Research, College of Science Research Center.

References

Barbieri, E.M.S., Lima, E.P.C., Cantarino, S.J., Lelis, M.F.F., Freitas, M.B.J.G., 2014. J. Power Sources 269, 158.
Cao, L., Xu, F., Liang, Y., Li, H., 2004. Adv. Mater. 16, 1151.
Chang, J., Mane, R., Ham, D., Lee, W., Cho, B., Lee, J., Han, S., 2007. Electrochim. Acta 53, 695.
Chang, J., Wu, C., Sun, I., 2010. J. Mater. Chem. 20, 3729.
Chang, K., Hu, C., 2004. J. Electrochem. Soc. 151, 958.
Goldbarger, J., He, R., Zhang, Y.F., Lee, S., Yan, H., Chol, H.J., Yang, P., 2003. Nature 422, 599.
Gulino, Tabbi, G., Scalisi, A., 2003. Chem. Mater. 15, 3332.
Gupta, V., Kusahara, T., Toyama, H., Gupta, S., Miura, N., 2007. Electrochem. Commun. 9, 2315.
Im, S., Lee, Y., Wiley, B., Xia, Y., 2004. Angew. Chem. Int. Ed. 44, 2154.

Jia, T., Wang, W., Long, F., Fu, F., Wang, H., Zhang, Q., 2009. J. Phys. Chem. C 113, 9071.
Kim, H., Horwitz, J.S., Kim, W.H., Makinen, A.J., Kafafi, Z.H., Chrisey, D.B., 2002. Thin Solid Films 420, 539.
Kondo, R., Okimura, H., Sakai, Y., 1971. Jpn. J. Appl. Phys. 10, 1547.
Li, X., Gao, H., Murphy, C., Gou, L., 2004. Nano Letters 4, 1903.
Li, Y., Tan, B., Wu, Y., 2008. Chem. Mater. 20, 567.
Liao, M., Liu, Y., Hu, Z., Yu, Q., 2013. J. Alloys Compd. 562, 106.
Ou, F., Buchholz, D., Yi, F., Liu, B., Hseih, C., Chang, R., Ho, S., 2011. ACS Appl. Mater. Interfaces 3, 1341.
Pan, Z., Dai, Z., Wang, Z., 2001. Science 291, 1947.
Pawar, B.N., Ganesh, T., Ham, D., Mane, R.S., Ghule, A., Sharma, R., Jadhav, K.D., Han, S.H., 2009. Sol. Energy Mater. Solar Cells 93, 524.
Tao, F., Shen, Y., Liang, Y., Li, H., 2011. J. Solid-State Electrochem. 11, 853.
Waghulade, R.D., Patil, P.P., Pasricha, R., 2007. Talenta 72, 594.
Wang, Y., Wang, H., Wang, X., 2013. Electrochim. Acta 92, 298.
Wang, W.S., Zhen, L., Xu, C.Y., Shao, W.Z., 2008. J. Phys. Chem. C 112, 14360.
Wang, X., Li, Y., 2002. Angew. Chem. Int. Ed. 41, 4790.
Wu, Q., Xu, Y., Yao, Z., Liu, A., Shi, G., 2010. ACS Nano 4, 1963.
Xia, X.H., Tu, J.P., Wang, X.L., 2011. Chem. Commun. 47, 5786.
Xu, C., Li, B., Du, H., Kang, F., Zeng, Y., 2008. J. Power Sources 180, 664.
Yang, Y., Jin, S., Medvedeva, J., Ireland, J., Metz, A., Ni, J., Hersam, M., Freeman, A., Marks, T., 2005. J. Am. Chem. Soc. 127, 8796.
Yang, H., Zeng, H., 2004. Angew. Chem. Int. Ed. 43, 5930.
Yuan, C.Z., Hou, L.R., Shen, L.F., 2010. Electrochim. Acta 56, 115.
Yu, D., Yam, V., 2004. J. Am. Chem. Soc. 126, 13200.
Zhao, T., Jiang, H., Ma, J., 2011. J. Power Sources 196, 860.
Zhang, Y-Q., Xia, X-H., Kang, J., Tu, J-P., 2012. Chin. Sci. Bull. 57, 4215.

Please cite this article in press as: Tehare, K.K. et al., Electrochemical supercapacitors of cobalt hydroxide nanoplates grown on conducting cadmium oxide base-electrodes. Arabian Journal of Chemistry (2017), http://dx.doi.org/10.1016/j.arabjc.2016.01.006